Journal of Wind Engineering and Industrial Aerodynamics, 6 (1980) 207—225

A WIND TUNNEL STUDY OF THE MEAN PRESSURE FORCES ACTING ON LARGE GROUPS OF LOW-RISE BUILDINGS

M. HUSSAIN

University of Engineering and Technology, Lahore (Pakistan)

B.E. LEE

Department of Building Science, University of Sheffield, Sheffield S10 2TN (Gt. Britain)

(Received June 8, 1979, accepted in revised form December 18, 1979)

Summary

The assessment of the wind pressure forces acting on low-rise buildings in urban and suburban areas is dependent on an understanding of the complex flow phenomena in an inner region of the atmospheric boundary layer close to the surface of the earth. As a result of these complexities the current design methods which attempt to predict such forces, for either wind loading or natural ventilation purposes, tend to over-simplify the assessment problem and can lead to inaccurate estimates.

Whilst the few studies reported previously in the literature demonstrate that the proximity effects of buildings grouped together can affect the values of their surface pressure coefficients, too often simplified design procedures take the form of a correction factor applied only to a design wind speed whilst the pressure coefficients to which this speed is applied remain based on the results of tests on isolated bodies.

The purpose of this paper is to present the results of a series of wind tunnel tests in which the surface pressure fields of low-rise buildings have been studied. These tests start with an examination of how the body shape influences the surface pressures for a range of isolated bodies. The test results then go on to describe how the parameters which describe an array of such model buildings influence the surface pressures. Both the body form and the array form have been widely varied in order to formulate design information which covers a practical range of built form planning requirements.

The results presented here demonstrate that it is possible to describe the surface pressures on groups of low-rise buildings in terms of three types of flow regime known to exist for the flow over general arrays of roughness elements on a surface.

1. Introduction

The state of our knowledge of the structure of the wind and its effects on buildings can sometimes have limiting effects on the design of tall structures, particularly where human susceptibility to vibration is concerned. This situation is rarely applicable to low-rise buildings, often housing units, where the limiting factors are more likely to be those associated with economic construction processes. With less incentive to investigate, the result is that our knowledge of the way pressure forces occur on low-rise buildings is relatively

poor, particularly where the effects of the proximity of one such building to another are concerned. Indeed, during the final discussion session at the Fourth International Conference on Wind Effects on Buildings and Structures, Harding [1] made a plea that a wind loading code should be produced principally for the benefit of low-rise structures, since these involve the majority of the building construction budget, and to which the majority of all wind damage occurs.

The purpose of this paper is to report the results of a wind tunnel study of the pressure forces on low-rise buildings and the way in which they are influenced by the shape of the building itself and the form of the pattern, or array, in which large groups of such buildings may be arranged. This study has attempted to cover the ranges of both building form and group array form which apply to typical full-scale situations; a detailed study of the factors which describe these form parameters is given by Soliman and Lee [2].

In a previous paper, Lee and Soliman [3] reported a study of the mean, wind-induced, pressure forces on arrays of cube-type roughness elements immersed in a turbulent boundary layer. This initial study was successful in that it appeared to confirm that the existence of three types of flow regime, associated with different element layout patterns, was applicable to three-dimensional bodies. This regime classification, first suggested by Morris [4], of isolated roughness flow, wake interference flow and skimming flow, had previously only been identified in connection with two-dimensional roughness elements. However there were a number of criticisms of this work and its potential application to the problems of wind effects on arrays of low-rise buildings. These criticisms, which concerned both the range of building forms tested and the characteristics of the incident flow, have been accepted as having some validity, and as a result, the more detailed investigation to be presented here has been undertaken. The authors now consider that the critical issues have been resolved and that the data contained in this paper have an application to building aerodynamics.

The importance of understanding how the flow effects which influence a low-rise building are modified by its presence in a large group of similar buildings is not restricted to loading code considerations. The distribution of external pressure forces will also govern the wind-induced natural ventilation characteristics of buildings. Such natural ventilation rates play an important role in determining both the internal comfort conditions of a building as well as its space heating energy demands. This latter consideration is becoming of increasing significance; as buildings become better thermally insulated a greater proportion of the heating demand is required to satisfy heat losses associated with air infiltration. Within the regime of ventilation design, perhaps more so than that of loading codification, the information available to the designer is not adequate for the proper execution of his task and the need for a clearer understanding of the wind forces on buildings in urban and sub-urban areas is paramount.

2. The experimental procedure

Full details of the experimental procedure and of its results can be found in Hussain [5].

2.1 The wind tunnel and incident flow

The series of experimental tests, to be described here, were conducted in the Sheffield University 1.2 × 1.2 m Boundary Layer Wind Tunnel. Details of the design, construction and operation of this wind tunnel in the format in which it existed over the test period are given in Lee [6]. The tunnel has since been rebuilt and now has a larger speed range. The working section, whose cross-section now measures 1.2 × 1.2 m, has a length of 7.2 m incorporating a 1.1-m diameter turntable whose center lies 5.4 m downstream of the entry position.

For the measurements to be reported here the incident flow consisted of a simulated atmospheric boundary layer wind appropriate to flow over urban terrain conditions. This incident flow was subsequently modified by the flow characteristics produced by a particular model array layout pattern in the immediate vicinity of an instrumented central model. The compromise between the size of the model array and the use of the simulated atmospheric flow apparatus is discussed later. The characteristics of the simulated urban atmospheric boundary layer are given in detail by Lee [6] and are summarised here

Depth of boundary layer = 800 m.
Power law exponent = 0.28.
Scale ratio (spectral method) 1:350.

The method used for the production of the simulated boundary layer utilises the fence, spires and floor roughness element approach suggested by Counihan [7]. This use of Counihan's method has been shown by Lee [6] to give an adequate representation of both the mean velocity and turbulence characteristics of the urban atmospheric boundary layer.

2.2 The models

The roughness element array layouts utilised building models made of hardwood which surrounded a central instrumented model, machined from aluminium alloy. The central model was fitted with pressure tappings on one vertical face only such that it was necessary to rotate the model to obtain both windward and leeward pressure distributions and hence to evaluate the drag force from an integration of the pressure distribution measurements. Full details of the exact location of each of the pressure tappings on all of the 20 different models used in this investigation are given in Hussain [5]. Twenty-six tappings were located on each vertical face with eight along the vertical centreline. The central models were also fitted with seven tappings on the roof centreline. The model surface pressures themselves were measured using a Scanivalve pressure scanning switch fitted with a Setra Type 237 differential pressure transducer and also using a TEM multiple-tube tilting manometer.

The pressure datum was taken from the static pressure tube of a standard NPL-type pitot-static tube situated in the free stream vertically above the central model. This pitot-static tube also provided a measurement of the dynamic head used to non-dimensionalise the surface pressures and was coupled to a Betz manometer in addition to the TEM instrument. The measurements of flow velocity used in the velocity profile analysis, referred to later, were made with a DISA Series M Hot Wire Anemometer System using straight, slant and X-array probes. All the measurements reported here are for the wind direction normal to the windward face.

The test programme was divided into a number of parts which utilised different model forms. The initial tests were performed with a cube-type building shape in order to check the earlier findings of Lee and Soliman [3] under the improved incident flow conditions which more adequately simulate the atmospheric boundary layer. The cube had a side length measurement of 36 mm, denoted by H, and contained 33 pressure tappings on one face and the roof. Mean pressure measurements were made on the windward and leeward faces and on the roof for 13 cases of element plan area density from 3.1% to 50%, with the elements arranged in both normal, grid iron, and staggered, checkerboard, patterns, where the remaining elements of the array were also 36 mm side length cubes. Mean velocity profile measurements were made for 8 values of the plan area density in the range 5—30% for the normal layout pattern only.

In the second and third phases of the investigation central models of various different plan forms were used, where in every case the model shape used for the array was the same as that of the instrumented model. The second series of tests used models having frontal aspect ratios of 0.5, 1.0, 1.5, 2.0 and 4.0 where in each case the side aspect ratio of these models remained square with a side length of 36 mm. Tests were carried out for the normal array pattern only over a range of 15 plan area densities from 2.5% to 60% for the mean pressure measurements and 7 plan area densities from 5% to 40% for the mean velocity profiles. The third series of tests covered the same range of layout pattern densities but were for models having side aspect ratios of 0.5, 1.0, 1.5 and 2.0 where again the front aspect ratio remained square with a 36 mm side length.

The fourth phase of the investigation was concerned with the effect of varying the height of the central model relative to that of the surrounding roughness element layout. The models used were square in horizontal cross-section with a side length of 36 mm and the surrounding elements of the array were 36 mm cubes. The relative heights of the different central models used were 0.5, 0.8, 0.9, 1.0, 1.1, 1.2, 1.3, 1.5, 1.7, 2.0, 3.0 and 4.0 times the cube height. Mean pressure measurements were made for array plan area densities of 5.0%, 6.25%, 12.5% and 25% in the normal layout pattern and 10%, 12.5%, 25% and 40% in the staggered layout pattern.

2.3 Isolated models

In addition to the phases of the investigation described in the preceding section a series of mean surface pressure measurements were carried out on each of the model shapes set in isolation in the centre of the turntable. In this series of tests the atmospheric boundary layer simulation apparatus remained in the forward part of the working section, with the exception of tests on the cube model in isolation, which was also tested in the empty tunnel subject only to the smooth wall boundary layer growth on the tunnel floor.

2.4 The effects of upstream fetch

Following the isolated model tests but prior to the tests on model arrays, a further phase of the investigation was conducted, in order to determine the influence of upstream fetch geometry on the model surface pressure distributions. The extremes of upstream fetch conditions were either that the particular model layout under test could be arranged to fill the entire length of the working section, 5.4 m upstream from the turntable centre, or that the general roughness array of the atmospheric boundary layer simulation apparatus could extend down to the immediate proximity of a very small particular array size. However it was felt that some compromise would exist whereby it was possible to have a sufficiently large array size to yield representative results and at the same time to have the correct general background to the flow field conditions that would be produced by the simulation apparatus. This part of the investigation, which utilised only the cube form of model, was conducted for plan area densities of 5%, 10%, and 20% in the normal layout pattern and 10%, 20% and 25% in the staggered layout pattern.

3. Results and discussion

3.1 Isolated models

Measurements of the mean surface pressure on the cube model in isolation were made both with the simulated atmospheric flow upstream as well as in the empty tunnel smooth wall boundary layer. A reduction in the mean pressures on both the side walls and the roof was apparent when the flow simulation was introduced, leaving a clear space of 25 H around the model. This resulted in a decrease in C_{D_1}, the drag coefficient based on the free stream velocity, from 0.65 to 0.28. This reduction is thought to be principally caused by the corresponding increase of the ratio of building height to boundary layer thickness from 4 to 22. When the mean drag coefficient, based on the velocity at the model roof height, C_{D_H}, was evaluated, values of 0.87 and 1.57 were obtained for the empty tunnel condition and the simulated boundary layer flow respectively. This latter value compares poorly with the value of 1.20 given by both the British Standard Code of Practice for Wind Loads, CP3 [8], and ESDU [9].

Using the range of models of various height ratios, isolated and with the

simulated flow upstream, the variations of mean drag, C_{D_H}, and mean roof uplift, C_{L_H}, were obtained as a function of their relative height, Fig. 1. This figure shows that the variation of both drag and lift forces with the increase of building height underwent an abrupt change at a value of $1.6H$. Below this critical height the reduction of both uplift and drag with height was pronounced, while above $1.6H$ both forces remained approximately constant. This graph may serve to distinguish between buildings with low-rise loading characteristics and those with high-rise characteristics. It is interesting to note that the trend exhibited in the drag variation for buildings in the height range $0.5H$—$1.6H$ is the reverse of that indicated by CP3 [8].

The variation of the drag coefficient, C_{D_1}, with aspect ratio for isolated models of various side aspect ratios and frontal aspect ratios is shown in Fig. 2. The variation in the drag with changes of frontal aspect ratio is minimal and has been shown by an examination of the pressure distributions to be due to the fact that changes in the base pressure are counteracted by changes in the windward face pressure, Hussain [5]. Figure 2 shows the drag force to have a greater dependence on the value of the side aspect ratio, particularly below a value of 1.5. This variation in drag is solely due to changes in the base pressure which reflects changes in the flow pattern as the "afterbody" length increases and alters the conditions for flow into the base cavity.

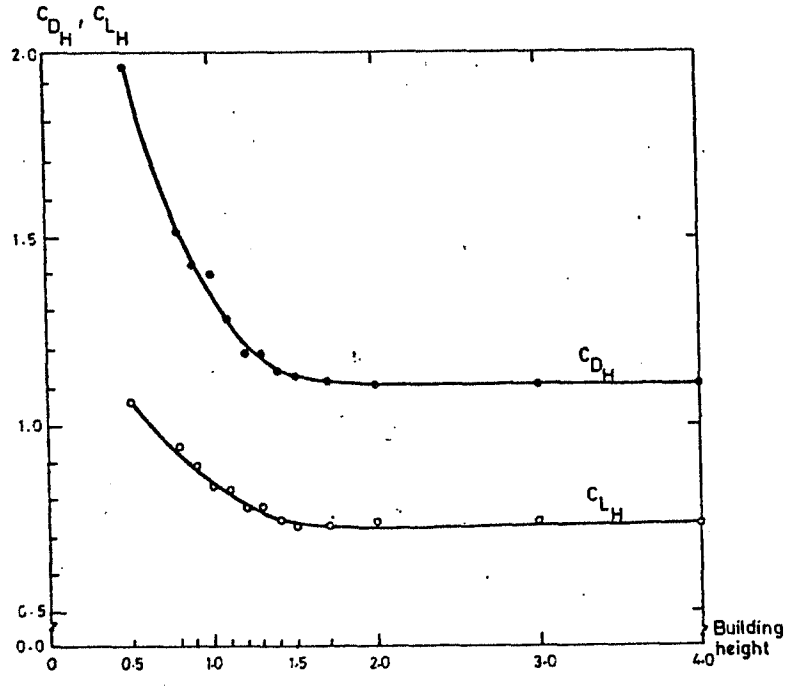

Fig. 1. The variation of drag and roof lift coefficients with building height for isolated models.

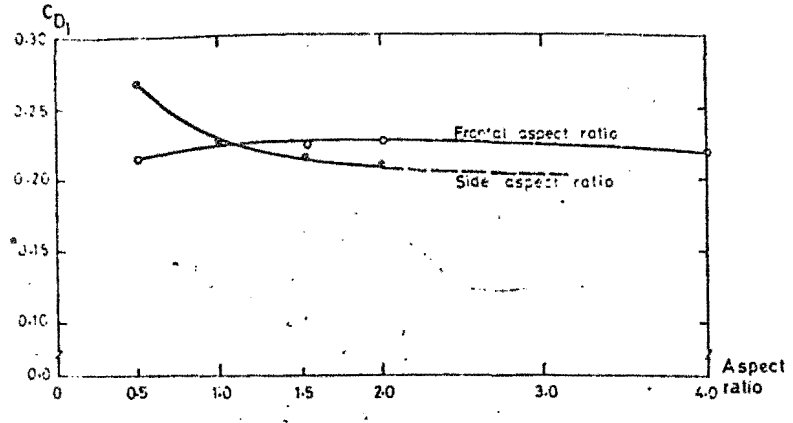

Fig. 2. The variation of drag coefficient for isolated buildings of different frontal and side aspect ratios.

3.2 The influence of upstream fetch

The reason for carrying out this part of the test programme was to determine the upstream fetch conditions which would permit mean pressure and velocity measurements to be made which would adequately reflect the influences due to model pattern and area density changes. The array size, denoted by R, could be varied in the range $3H$—$145H$ upstream, and $3H$—$25H$ downstream, of the instrumented model. The tests started by gradually extending the array size in the otherwise empty working section until the pressures measured on the surface of the instrumented model ceased to vary. At this point the pressures were considered to have stabilised.

Figure 3 shows the variation of the drag coefficient C_{D_1} with R/H for the various combinations of pattern and plan area density tested. It can be seen

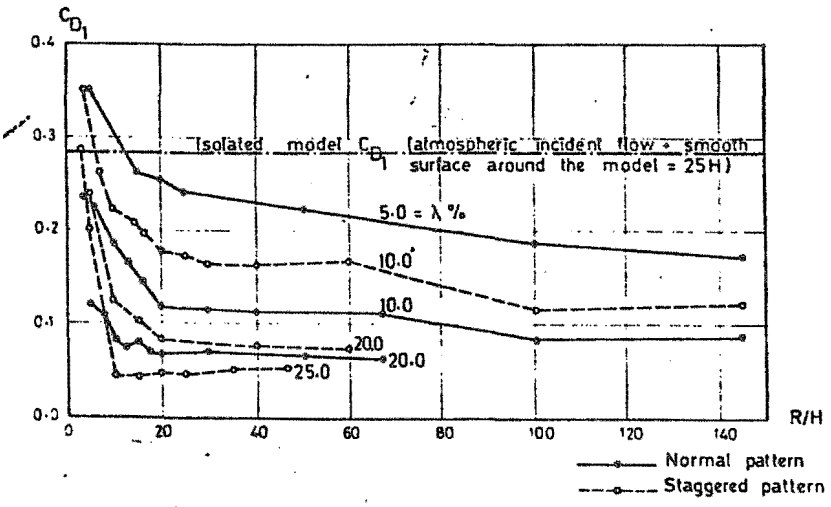

Fig. 3. The variation of drag coefficient with upstream fetch length for arrays of cubes.

that the rate at which the drag coefficient decreases as the fetch length is extended is dependent on the density and pattern of the array. The reduction is quite abrupt for the higher densities and more gradual for the low density arrays, where for the 5% normal pattern and 10% staggered pattern the majority of the reduction has occurred by $R = 25H$, and for the 20% normal pattern and 25% staggered pattern, by $R = 10H$.

Following this approximate assessment of the array fetch required for pressure stability the simulated atmospheric boundary layer apparatus was then introduced upstream. A further reduction in the value of C_{D_1} was then recorded for all the combinations of array pattern and density considered. Taking the 5% normal pattern as an example the values of C_{D_1} of 0.25 and 0.17 for array fetches of $25H$ and $145H$, respectively, fell to 0.15 when the simulation apparatus was introduced upstream of a pattern array size of $25H$. This reduction is considered to justify the use of a particular model array fetch of $25H$ for low density arrays reducing to $10H$ for the highest density arrays in the test programme. The simulation apparatus then remained in the forward part of the working section for the remainder of the test programme, extending downstream to meet the size of a particular model array.

The conclusion reached in this section has referred only to measurements of the drag coefficient; however, it could be equally well substantiated by reference to the roof uplift force coefficient results.

3.3 Cube-type building arrays

As stated in the Introduction to this paper the purpose of this phase of the study was to repeat the earlier investigation by Lee and Soliman [3] on the wind pressure forces on arrays of cube elements, but under more-rigorous incident flow conditions. The range of test parameters relevant to this phase of the investigation is described in Section 2.

One of the more important conclusions reached by Lee and Soliman [3], following the work of Morris [4] and Marshall [10], was that the variation of both the windward and leeward pressure coefficients, C_{p_w} and C_{p_b}, with element spacing, or plan area density, could be represented by a broken straight line. From this, it followed that the variation of the mean drag coefficient, C_{D_1}, with spacing for a particular type of layout pattern could also be represented by a broken straight-line relationship where the breaks, or inflections, were considered to reflect a change in the type of flow regime. This was considered as supporting evidence for the existence of Morris's three flow-regime categories in the flow over three-dimensional roughness elements. These flow regimes which are applicable to pipe flow, open channel flow and flat plate boundary layers are denoted as isolated roughness flow, wake interference flow and skimming flow. In the isolated roughness flow regime the roughness elements are sufficiently far apart that each element acts in isolation and behind each the wake and separation bubble develop completely, reattachment occurring before the next element is reached. In the second regime the roughness elements are close enough to each

other so that the separation bubble associated with each element does not have room to develop fully. In the third regime, the roughness elements are closer still so that stable vortices are created in the spaces between the elements. The flow here appears to skim on the crests of the elements.

Figures 4 and 5, which present the results of the present investigation, show the variation of C_{D_1}, C_{p_w} and C_{p_b} with element spacing ratio S/H, and plan area density λ, for the normal and staggered patterns, respectively. The trends of the variation of the pressure forces with element spacing depicted here are similar to those found by Lee and Soliman [3]. However in the present investigation the transition from one flow regime to another was not found to occur at a specific value of the element spacing ratio, S/H, but to occur with a finite range of spacing values. It was found that this transition region between flow regimes could be more clearly identified from values of the pressure forces taken from the element centreline tappings alone rather than those averaged over the element face as a whole.

From Figs. 4 and 5 the following conclusions are suggested:

(a) the isolated roughness flow regime exists for values of $S/H > 3.2$—3.6 for both layout patterns;

(b) the skimming flow regime exists for values of $S/H < 2.2$—2.6 for both layout patterns; and

(c) the wake interference flow regime occurs for average element spacing values between 2.4 and 3.4.

Furthermore, it is possible to substantiate these values for the flow regime limits by a flow pattern hypothesis based on other bluff body flow studies.

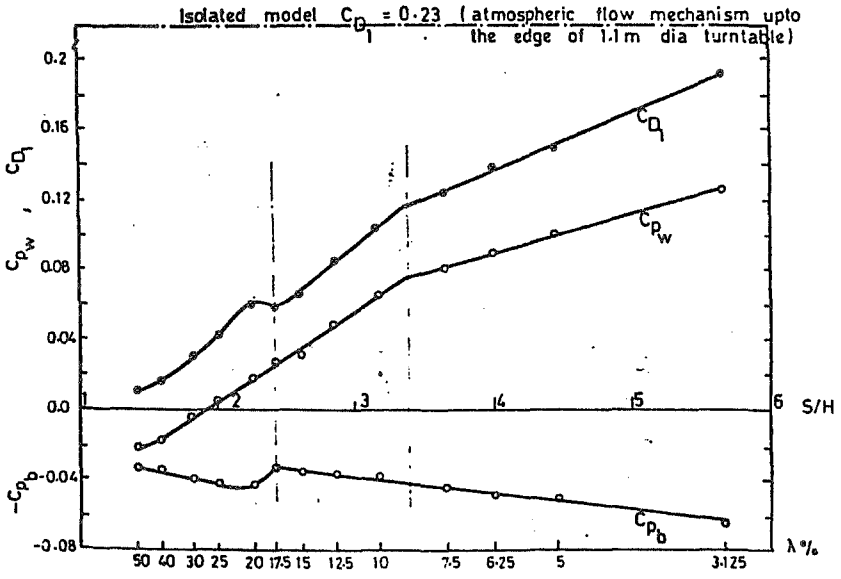

Fig. 4. The variation of wall pressures and drag coefficient with building spacing and plan area density. Cube arrays in the normal pattern.

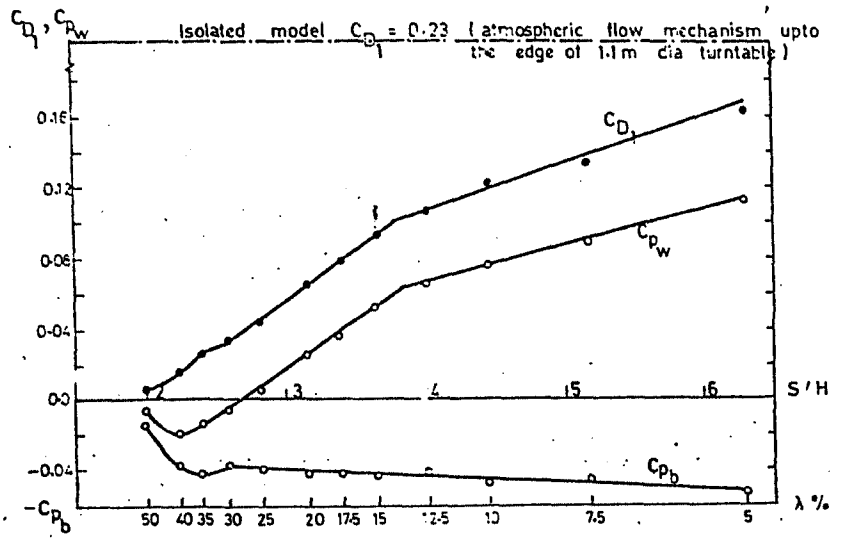

Fig. 5. The variation of wall pressures and drag coefficients with building spacing and plan area density. Cube arrays in the staggered pattern.

It is suggested that the lower limit of the isolated roughness flow regime would be reached at an element spacing equivalent to the total distance between the upstream separation point and the downstream reattachment point of the flow around an isolated cube. The figures given for these separated flow region lengths by Castro and Robins [11] of 0.9H and 1.5H, for the upstream and downstream distances respectively, together with the cube length itself of 1H, agree well with the value of 3.4H for the average lower limit of the isolated roughness flow regime found in the present study.

Similarly it is possible to arrive at an estimate for the upper limit of the skimming flow regime by considering the cavity size necessary for the establishment of a stable vortex. Tani et al. [12], in work on two-dimensional grooves in a smooth surface, estimated that the onset of a stable vortex condition occurs at a cavity length-to-height ratio of 1.4. When the length of the element, 1H, is added to this, the figure agrees well with the present results.

Figures 4 and 5 also show the value of the isolated element drag. A comparison of this value with those for the drag of grouped elements clearly illustrates the importance of proximity effects in the determination of wind pressure forces.

In this phase of the investigation the roof pressure distributions were also measured and were subsequently integrated to give the mean roof uplift force. An examination of the pressure distributions showed the point of maximum suction to be at the leading edge of the roof for all conditions of array pattern and density. Figure 6 shows the variation of the roof lift coefficient, based on the free stream velocity, C_{L_1}, with element spacing and plan area density. From this figure it can be seen that there is no apparent change in

format were restricted to the internal layer. A log–log plot of the velocity profile was used to measure the thickness of the internal layer. The graphical method proposed by Perry and Joubert [14] was used to derive values of the zero plane displacement, d, and the roughness length, Z_0, in the manner illustrated by Lee and Soliman [3].

The variation of the zero plane displacement ratio d/H with the equivalent frontal area density of the cube arrays is shown in Fig. 7, where the present results are compared with those of Counihan [15]. Exact agreement ought not to be expected here since Counihan's elements were not exact cubes, and, furthermore, he used an average value of d based on velocity profiles taken either side of the element centreline.

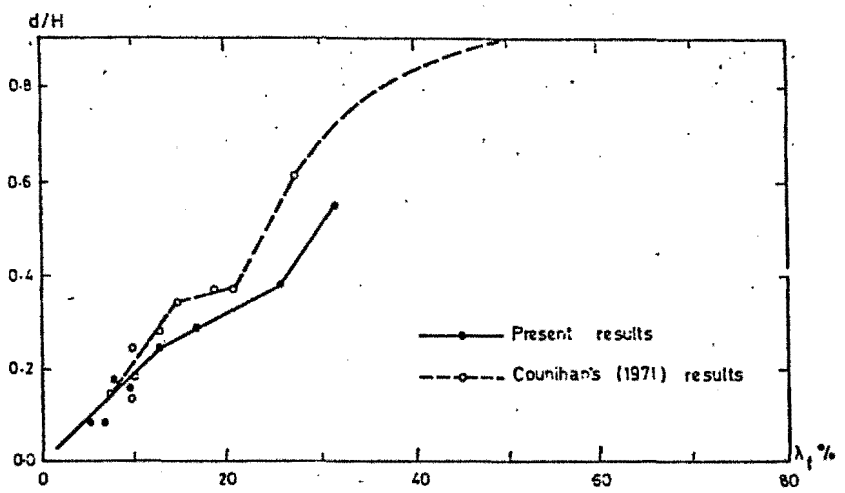

Fig. 7. The variation of zero plane displacement with frontal area density for cube arrays in the normal pattern.

3.4 Arrays of buildings of various frontal aspect ratios

A study of the surface pressures experienced by isolated buildings over a range of different frontal aspect ratios is reported in Section 3.1. This study has been extended to include measurements of the pressures on the same range of models where they now form part of a large array of identical buildings. No comparable study covering this range of parameters is known to the authors, though some flow visualisation results are available [16]. The ranges of the variables included in this phase of the investigation are given in Section 2.

The variation of the central element drag coefficient, C_{D_1}, with variations in array element spacing for the range of frontal aspect ratio models from 0.5 to 4.0 is shown in Fig. 8. When the values of the drag coefficients of the different models are compared with their corresponding isolated body values, Section 3.1, the significant reduction brought about by group proximity is apparent. Figure 8 also demonstrates that the inflections in the relationship

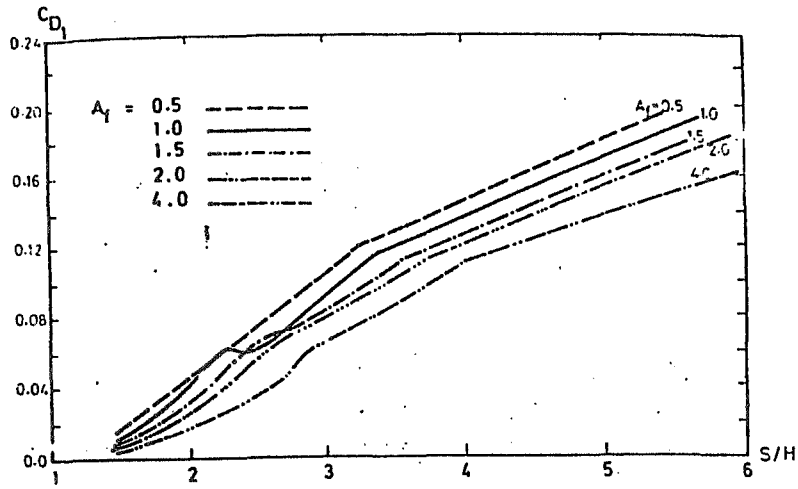

Fig. 8. The variation of drag coefficient with building spacing for arrays of different frontal aspect ratio models in the normal pattern.

between element drag and spacing ratio used to identify the limits of the three different types of flow regime for cube arrays, Section 3.3, are also applicable to arrays of other body shapes.

Using these inflection points to identify flow regime changes enables the conclusion to be drawn from Fig. 8 that the values of S/H at which the changes occur depends on the value of the bodies' frontal aspect ratio as well as the array configuration. Across the range of frontal aspect ratio from 0.5 to 4.0 it can be seen that the change of flow regime from isolated roughness flow to wake interference flow occurs at values of S/H which progress from 3.25 to 4.0, respectively. Similarly, the value of S/H at which the second change occurs, from wake interference to skimming flow, also increases from 2.30 to 2.55 across the same range of frontal aspect ratio models. It might well be expected that the frontal aspect ratio would have a large influence on the change from isolated roughness flow to wake interference flow since it has been suggested already that the lower limit of the former flow regime occurs when the total distance between the upstream separation point and downstream reattachment point of an isolated body of the same shape equals the array element spacing. The flow visualisation results of Evans [16] for a range of various isolated frontal aspect ratio models indicate that the downstream reattachment point varies continuously for frontal aspect ratio values of up to 10.0. Rather less influence of the variation of frontal aspect ratio on the second flow regime change might also have been expected since it has already been suggested that the upper limit of the skimming flow regime occurs at an element spacing compatible with the establishment of a stable cavity vortex. Previous studies of flow in slots and grooves [12] have shown that the vortex stability is more critically dependent on the groove height than on the groove width normal to the flow, and thus, in the present case,

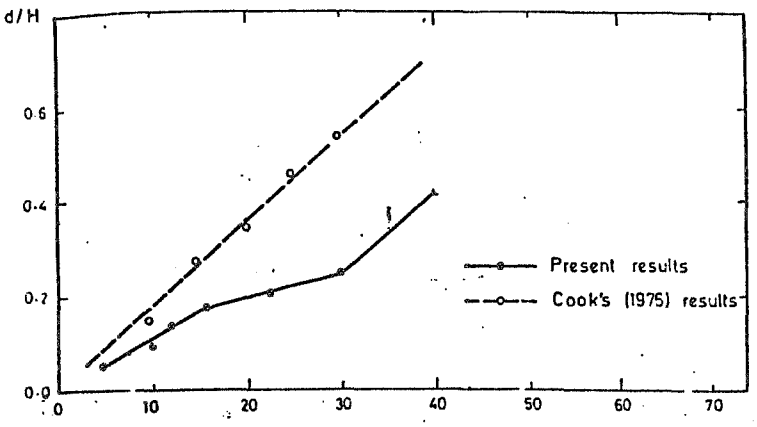

Fig. 10. The variation of zero plane displacement with frontal area density for arrays of frontal aspect ratio models of 2.0 in the normal pattern

same value of element spacing. This lower drag value implies that the corresponding value of the equivalent surface skin friction coefficient, used in the graphical determination of the zero plane displacement, will also be lower and that as a consequence d will be higher.

3.5 Arrays of buildings with various side aspect ratios

This phase of the investigation follows closely the format set out for the study of various frontal aspect ratio models described in Section 3.4. Here again no previous comparable tests were known to the authors. The range of parameters studied in this phase, given in Section 2, only includes the normal element array pattern and does not include any velocity profile measurements.

Figure 11 shows the variation of the element drag coefficient, C_{D_1}, with

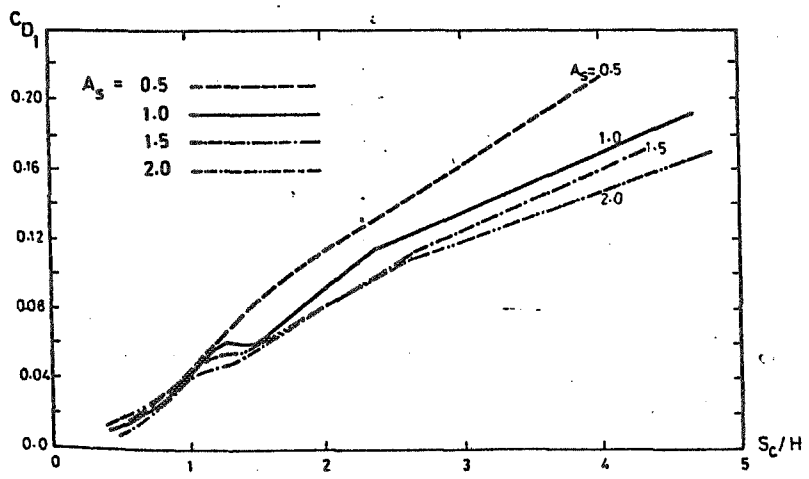

Fig. 11. The variation of drag coefficient with building spacing for arrays of different side aspect ratio models in the normal pattern.

element spacing for values of the side aspect ratio of 0.5, 1.0, 1.5 and 2.0. Here, the element spacing referred to is the clear spacing between elements in the flow direction, S_c, and not the element centre spacing, S, as used in previous sections, since for this type of element form the body length varies in the flow direction as the side aspect ratio varies. Figure 11 again indicates the dramatic reductions in drag brought about by group proximity effects over the isolated body drag values given in Section 3.1. The order of magnitude of the reduction in drag for side aspect ratio body arrays shown here, is the same as that for the frontal aspect ratio arrays shown in Fig. 8.

The inflection points in the rate of reduction of element drag with reduced spacing have again been used to identify changes of flow regime. The first change, from the isolated roughness to wake interference flow, occurs at values of S_c/H varying from 2.1 to 2.6 as the side aspect ratio is increased from 0.5 to 2.0. The second change, from wake interference to skimming flow, occurs at a constant value of S_c/H of 1.4 for all element side aspect ratio array values.

An examination of the behaviour of the leeward face pressure coefficient variations with element array density for the range of model forms has shown that different trends were apparent between the 0.5 side aspect ratio model and the remainder of the group and that the trends for this particular low side aspect ratio model bore a resemblance to those for the 2.0 and 4.0 frontal aspect ratio models [5]. The explanation offered for the leeward face pressure coefficient behaviour concerns the flow into the base cavity resulting from a situation in which the flow does not reattach itself to the element sides.

The base pressure variation with element array density for bodies with side aspect ratios of 1.5 and 2.0 was found to be similar to that observed the case of the 0.5 frontal aspect ratio shaped body. In these cases it is suggested that, by virtue of their long afterbody shape, the flow reattaches on the roof and sides of the models. Due to this flow reattachment, the shear layers, which feed the base cavity vortex, are deflected outwards and thus the core of the vortex forms further downstream than if sidewall flow reattachment had not occurred. The downstream limit of this vortex position will then be defined by the position of the next roughness element in the array. In such a situation, when the spacing between the elements is progressively reduced, the vortex is pushed nearer and nearer to the rear face of the model, causing the flow pattern and thus the base pressure to vary progressively. This hypothesis would then explain the observation that for all such long afterbody models the leeward pressures vary as the spacing varies, up to the start of the skimming flow regime. A comparison of horizontal pressure distribution across the width of the leeward face normal to the flow, between short and long afterbody models, tended to confirm this hypothesis, where the short model pressure distributions exhibited a pronounced peak due to the proximity of the vortex whilst the long model pressure distributions remained constant.

ed roughness and wake interference flow regimes. Of more importance to the present study, however, Joubert et al. investigated one specific case of a three-dimensional element array layout using cuboid roughness elements in a staggered, 8% plan area density array. Their central model had a 3:1 horizontal side aspect ratio with its wider side normal to the flow and they reported that its drag coefficient, C_{D_1}, showed a linear increase with increases in its height.

The variation of the centreline drag coefficient based on the free stream velocity, C_{DC}, with central model height is shown in Fig. 13 for a range of

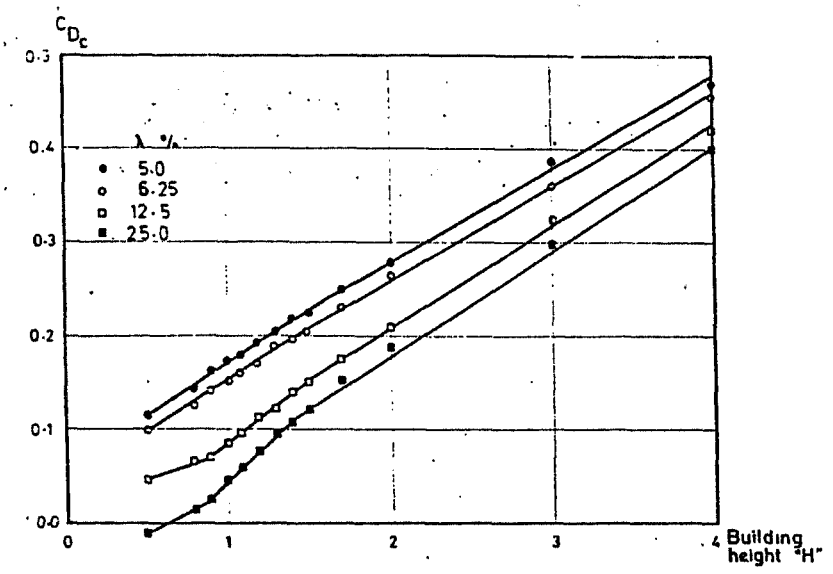

Fig. 13. The variation of drag coefficient, C_{D_1}, with building height for models surrounded by various cube arrays.

array densities in the normal layout pattern. The trends in the drag variation depicted here are those of a broken straight line, whose inflection lies in the range $1.35H$—$1.60H$. For values of the model heights above the inflection points the drag variation lines are parallel for all array types, but below these points the lines diverge to show different trends between the different flow regimes. These inflection points are considered to divide the variation of drag with central element height into an outer zone and an inner zone. In the outer zone the variation of the drag is thought to be dependent on the flow in the outer part of the boundary layer, which, for all array types, will be governed by the simulated atmospheric boundary layer. This common incident flow field will then result in a similar variation of drag with height, but based on different starting points dependent on the extent of the inner zone. In the inner zone the wall pressures on the central element will be governed by the inner boundary layer growing on a particular element array layout, thus accounting for the variation in drag behaviour between flow regime array types observed here.

Conclusions

This paper has attempted to demonstrate, by means of a rigorous model analogue technique, that the proximity effects due to the construction of low-rise buildings in group arrays are important in the determination of wind-induced surface pressure forces. These proximity effects are apparent at very low building planning densities and cannot be adequately compensated for by model tests on isolated buildings in simulated atmospheric boundary layers, which reflect only the general characteristics of a particular terrain category.

References

1 L. Harding, Discussion Session 8, Proc. 4th Int. Conf. Wind Effects on Buildings and Structures, Heathrow, London, Sept. 1975.

2 B.F. Soliman and B.E. Lee, Some aspects of density and form relevant to air flow in urban areas, Build International, 7 (1974) 451—473.

3 B.E. Lee and B.F. Soliman, An investigation of the forces on three dimensional bluff bodies in rough wall turbulent boundary layers, Trans. A.S.M.E. J. Fluid Eng., 99 (1977) 503—510.

4 H.M. Morris, Flow in rough conduits, Trans. A.S.C.E., 120 (1955) 373—398.

5 M. Hussain, A study of the wind forces on low rise building arrays and their application to natural ventilation design methods, Ph.D. Thesis, Department of Building Science, Sheffield University, 1979.

6 B.E. Lee, The simulation of atmospheric boundary layers in the Sheffield University 1.2 x 1.2 m boundary layer wind tunnel, Proc. 3rd Colloq. Ind. Aerodyn., Fachhochschule Aachen, F.D.R., June 1978.

7 J.C. Counihan, Simulation of an adiabatic urban boundary layer in a wind tunnel, Atmos. Environ., 7 (1973) 673—689.

8 British Standards Institution, Code of Practice 3, Chapter 5, Part II, Wind Loads, London, 1972.

9 E.S.D.U., Fluid forces, pressures and moments on rectangular blocks, Engineering Societies Data Unit, Item 71016, London, Sept. 1971.

10 J.K. Marshall, Drag measurements in roughness arrays of varying density and distributions, J. Agric. Meteorol., 8 (1971) 269—292.

11 I. Castro and A. Robins, The flow around a surface mounted cube in uniform and turbulent streams, J. Fluid Mech., 79 (1977) 307—335.

12 I. Tani, M. Iuchi and H. Komoda, Experimental investigation of flow associated with a step or a groove, Rep. No. 364, Vol. 27, Aeronautical Research Institute, University of Tokyo, 1961.

13 B.F. Soliman, A study of the wind pressure forces acting on groups of buildings, Ph.D. Thesis, Department of Building Science, University of Sheffield, 1976.

14 A.E. Perry and P N. Joubert, Rough wall boundary layers in adverse pressure gradients, J. Fluid Mech., 17 (1963) 193—211.

15 J.C. Counihan, Wind tunnel determination of the roughness length as a function of the fetch and roughness densities of three dimensional roughness elements, J. Atmos. Environ., 5 (1971) 637—642.

16 B.H. Evans, Natural airflow around buildings, Texas Eng. Expt. Res. Stn., Rep. No. 59, 1957.

17 N.J. Cook, Data for wind tunnel simulation of the adiabatic atmospheric boundary layer, Bldg. Res. Establ., Note N - 135/76, 1976.

18 P.N. Joubert, A.E. Perry and L.K. Stevens, Drag of a bluff body immersed in a rough wall boundary layer, Proc. 3rd Int. Conf. Wind Effects on Building Structures, Tokyo, 1971.